AN ABSTRACT OF THE THESIS OF

Michael Alexander Rodriguez for the degree of Master of Science in Chemical Engineering presented on June 9, 2020.

Title: Signal Enhancement in Lateral Flow Tests for Infant HIV Diagnosis.

Abstract approved: _____

Elain Fu

Paper-based assays for HIV diagnosis are cheap, portable, and require little to no skilled training, electricity, or expensive equipment to perform successfully. However, there is a need for tests with lower limits of detection (LOD) for diagnosing infection at the earliest stages. Effective labeling to increase signal-to-noise ratio is critical to achieving comprehensive early stage HIV detection and would also enable a reduction in the required patient sample volume. Our aim is to assess the LOD of sandwich-format lateral flow assays with localized geometric manipulations along the fluidic flow path and with various labeling schemes, including gold nanoparticles, black cellulose nanoparticles, and enzymatic amplification via *horseradish peroxidase* (*HRP*) with colorimetric substrate diaminobenzidine. Premixed and sequential reagent additions produced comparable results, so the premixed mode was selected as preferred due to its shorter time to result. Geometric constrictions offered marginal signal gains with a model system but did not offer similar improvements with our HIV system. The LOD achieved with the enzyme-based labeling scheme (approximately 10 pg/mL) and with cellulose nanoparticles (150 pg/mL) were substantially lower than the LOD achieved using conventional gold nanoparticles (19 ng/mL).

© Copyright by Michael Alexander Rodriguez
June 9, 2020
Creative commons license

Signal Enhancement in Lateral Flow Tests for Infant HIV Diagnosis.

by
Michael Alexander Rodriguez

A THESIS

submitted to

Oregon State University

in partial fulfillment of
the requirements for the
degree of

Master of Science

Presented June 9, 2020
Commencement June 2021

Master of Science thesis of Michael Alexander Rodriguez presented on June 9, 2020.

APPROVED:

Major Professor, representing Chemical Engineering

Head of the School of Chemical, Biological, and Environmental Engineering

Dean of the Graduate School

I understand that my thesis will become part of the permanent collection of Oregon State University libraries. My signature below authorizes release of my thesis to any reader upon request.

Michael Alexander Rodriguez, Author

TABLE OF CONTENTS

Chapter title	Page
1 Introduction...	1
A. Microfluidic driving forces	3
B. Lucas-Washburn flow	4
C. Darcy flow	5
D. Immunoassays	5
E. Kinetics	6
2. Signal enhancement by geometric manipulations	8
A. Introduction and background	8
B. Methods and materials	10
i. Reagent information	10
ii. Lateral flow strip processing	11
iii. Data analysis	12
C. Results and discussion	13
i. Localized constrictions; signal gains for model antibody system	13
ii. Localized constrictions; signal gains for HIV system	15
3. Detection of p24 antigen with colorimetric particles	16
A. Introduction and background	16
B. Materials and methods	18
i. Reagent information	18
ii. Cellulose nanobead label conjugation	19
iii. Lateral flow strip processing	19
iv. Data processing	20
v. Calculations: Limit of detection	21
C. Results and discussion	22
4. Detection of p24 antigen with horseradish peroxidase	25
A. Introduction and background	25
B. Methods and materials	26
i. Reagent information	26
ii. Assay sequence	27
C. Results and discussion	28
Bibliography	37

LIST OF FIGURES

Figure Page

1. “Schematic of model assay sandwich”…….……..... 9

2. “Schematic of fully assembled lateral flow assay card” …….….11

3. “Localized geometric constriction…model system” …….…..13

4. “Localized geometric constrictions…customized cellulose nanobead label” .…14

5. “Schematic of HIV stack with streptavidin-gold labeling” …….……16

6. “Schematic of HIV stack with CNB labeling” …….……...17

7. “Signal response curves for particle detection methods in HIV p24 assay” …...22

8. “Schematic of HIV stack with HRP amplification” …….……...25

9. “Signal improvements from reduction of detection antibody load” …….……..28

LIST OF TABLES

Table Page

1. “Assay component addition sequence for model stack with streptavidin-gold label” …… 12

2. “Assay component addition schedule for HIV assay with gold labeling” ……..…… 20

3. “Assay component addition sequence for HIV assay with… HRP amplification” …..…….. 27

LIST OF EQUATIONS

Equation Page

1. Reynold's number …… 3

2. Lucas-Washburn flow …….. 4

3. Darcy flow …… 5

Chapter 1: General overview and background

As of 2018, there are approximately 1.1 million children worldwide infected with the human immunodeficiency virus (HIV) with 160,000 new infections annually. (UNICEF, 2019) Antiretroviral drug treatment alone has reduced the mortality caused by HIV and AIDS by 20 % between the years 2005 and 2009. (United Nations Programme on HIV/AIDS (UNAIDS), 2010) These antiretroviral treatments must be implemented as early as possible to be effective. This makes early detection critical to improving the health outcomes of infected individuals. One of the earliest markers of HIV infection, p24, shows up approximately two weeks from the time of infection and remains detectable up to six weeks. (Routy et al., 2015) This makes p24 an ideal target candidate for early-stage HIV diagnosis.

In this study, we developed an assay to detect low concentrations of p24 protein in human plasma samples. P24 is a hexameric structural protein that comprises the inner shell of the virus. There are approximately 2,000 molecules per viral shell and has a molecular weight of 24 kDa. (Lin et al., 2012) Many commercial lateral flow methods for detecting HIV require the development of antibodies in response to infection, which can take approximately six weeks. Infants present a unique challenge to detect p24 due to the formation of immunocomplexes around the virus by maternal antibodies present in infants, thus masking our protein target. (Rich et al., 1997) In native samples this immune complex can be disrupted by applying heat or with an acid treatment prior to processing the sample on the matrix. Although not the scope of this study, sample pre-treatment to disrupt immunocomplexes around p24 complement the development of this early-stage detection.

One of the most common clinical assays used to diagnose HIV infection is the enzyme linked immunosorbent assay, or ELISA. ELISA is a diagnostic technique performed in a well-

plate and quantified using a UV-Vis spectrophotometer. These commercially available ELISAs can detect 5–25 pg/mL of p24 antigen on average. (Miedouge et al., 2011) ELISA is performed in a laboratory setting, requires skilled operators to execute the assay properly, requires dedicated laboratory equipment such as refrigeration, storage facilities, and other expensive or non-portable equipment. While there are ELISAs for p24 detection, these assays are ultimately not suitable for environments that lack these kinds of resources–low resource settings–which limit timely diagnosis as well as access to health services.

Low resource settings can be defined as areas where key health care resources—financial resources, human resources, and technical infrastructure—are not available or easily accessed. (Fritz et al., 2015) Examples of these settings can range from developing countries, remote locations, and the average household.

Point-of-care diagnostic paradigm

Point-of-care (POC) diagnostics brings these diagnostic technologies directly to the patient. In traditional diagnostic models, patients and testing are usually decoupled with insurance providers, testing facilities, and physicians and clinics acting in between. This results in long wait times and high expenditure of resources. Delivering diagnostic technology directly to the patient can shorten the time for diagnosis and provides the patient with earlier treatment options. ASSURED are criteria established by the WHO to which ideal POC devices should strive. (WHO, 2015) (Gomez et al., 2018) It must be, namely: affordable, sensitive, specific, user-friendly, rapid and robust, and deliverable to end-users (portable).

Our POC device uses nitrocellulose, a porous paper-like material that can transport liquid via capillary action. This matrix can be approximated as a series of monodispersed, uniform microscopic capillaries. (Peters & Durner, 2008) Flow properties of this matrix are critical to the

performance and optimization of lateral flow tests (LFTs). Paper-based POC devices have shown significant promise because they are portable, inexpensive, disposable, and have the ability to wick fluid via capillary action eliminating the need for external pump and valves. (Martinez et al., 2010)

A. Microfluidic driving forces

The flow velocities in LF strips exhibit laminar flow behavior, meaning that mixing is driven by diffusion, eliminating the need for external pumps and valves in a LFT. The Reynolds number (**Equation *1***) is a dimensionless measure of which forces drive fluid flow in a specific fluid. Those forces can be inertial, relating to the lateral velocity of fluid flow and the length traveled; or viscous, which characterizes the behavior at the interface between fluid and the porous surface.

$$Re = \frac{uD}{\nu} = \frac{inertial\ forces}{viscous\ forces}$$

Equation 1. *Reynold's number. Dimensionless ratio used to characterize flow regimes.*

where u is defined as the flow velocity of the fluid front [m/s], D is the average capillary pore diameter [m], and ν is the kinematic viscosity of the fluid [m^2/s].

Operating in the laminar flow regime provides unique capabilities to both mix two components directly on the matrix via a conjugate pad in the flow path and to maintain distinct packets of components traveling along the flow path. (Whitesides et al., 1999) That is, we can perform complex operations—mixing and discrete transfer—on the porous matrix by virtue of the flow regime at which we operate. In turbulent flow (Re>>1) discrete transfer is significantly challenging to achieve if sequential delivery of specified reagents is needed. A Reynold's

number less than 1 indicates that viscous forces dominate the flow regime, and flow behavior is laminar. The flow regime in our porous matrix has a Reynold's number, Re = 0.01. Typical conditions in our porous matrix include u = 0.2 cm/s, ν = 0.3 x10^-6 m^2/s, and D = 0.45 μm.

B. Washburn flow

When wetting out a dry substrate, fluid flow displacement is modeled by the Washburn equation. The wetted flow path length is proportional to the square root of the physical forces between fluid and substrate relative to the internal viscous forces of the flowing fluid. (Washburn, 1921) The Washburn equation (**Equation *2***) is modeled as follows:

$$L = \sqrt{\frac{\gamma d t}{4\mu}}$$

Equation 2. *Lucas-Washburn equation. Length quantity that indicates the fluid flow front pathway as a function of microscale forces and time.*

where L is the length of wetted material, γ is the surface tension at the air-fluid interface, d is the average pore diameter of the matrix, t is the time for the fluid front to wet out a dry membrane, and μ is the fluid viscosity.

Lucas-Washburn flow is critical when optimizing the performance of LFTs since most end-user devices involve the one-time addition of a liquid sample to a dry porous nitrocellulose matrix. Being able to predict the wet-out behavior of a LFT helps optimize for critical details such as regent mixing times; the time it takes for the fluid front to reach a test line or control line, which influences the positioning of immobilized assay components; and the time it takes for the device to fully wet out at the terminal end, which influences the dimensions of the porous matrix itself.

C. Darcy flow

Fluid flow continues even after the matrix has become fully wetted due to a highly absorbent cellulose material placed immediately at the terminal end of the lateral flow strip. This maintains a fluidic potential gradient that continues to draw liquid through the matrix via capillarity. The resulting changes in flow behavior are modeled more appropriately by a derivation of Darcy flow equation (Mendez et al., 2010):

$$Q = -\Delta P \frac{\kappa A}{\mu L}$$

Equation 3. *Darcy flow equation as a function of capillary pressure and fluidic properties*

Where Q is the volumetric flow rate, ΔP is the pressure gradient along wetted matrix, μ is fluidic viscosity, L is the length of matrix, κ is the permeability of matrix, and A is the cross-sectional area perpendicular to flow path in total matrix. Assays in this study with more complex addition sequences, such as enzymatic amplification, in fact operate in Darcy flow regime.

D. Immunoassays

This study focuses primarily on lateral flow immunoassays, a class of assay that takes advantage of the high binding affinities of antibodies to capture targets of interest, most commonly proteins. Specifically, the immunoassays studied in this document target the structural protein of the HIV capsid, p24. The structure of the antibody provides more insight into why they are so often used for assays and what is responsible for their high sensitivities.

Antibodies are protein secreted from the immune system to detect specific antigens in the body. These antigens can be foreign bodies such as viruses, bacteria, and foreign objects. The antibody is composed of a conserved region (Fc fragment) that provides an anchor for the variable region of the antibody, the Fab fragment. This variable region of the antibody expresses

a specific sequence, a paratope, responsible for binding between it and the complimentary sequence expressed on the antigen, the epitope. (M. Chiou et al., 2019)

There are two main categories of immunoassay types: competitive and direct detection. Competitive assays involve the displacement of a labeled binding pair by the more affinitive target antigen. (Slagle & Ghosn, 2018) The intensity of the labeled test line is inversely proportional to the amount of analyte present in the sample: higher analyte concentration yields a lighter signal. Competitive immunoassays are suitable for small molecules that may not bind as effectively to immobilized capture antibodies. Direct detection in immunoassays involves the direct capture of a target and the subsequent or simultaneous labeling of the captured target with a antibody label conjugate. In this assay, the signal intensity is directly proportional to the amount of analyte captured. Briefly, an immobilized antibody captures a target of interest. The captured analyte can then to directly labeled with a antibody label conjugate (direct detection) or with a secondary antibody that is then labeled by a colorimetric reagent (indirect detection). We explore both types of direct detection with gold nanoparticles and cellulose nanoparticles.

E. Kinetics

While the type of assay can be tailored for a detection scheme, ultimately binding kinetics determine the true efficiency and execution of your assay. The binding strength of an antibody-antigen pair is often characterized by the equilibrium dissociation constant (K_d). The dissociation constant can give us a general assessment of the binding and dissociation rates relative to each other, but it does not provide a broader assessment of antibody-antigen interactions, especially on short time scales. Two antibody-antigen pairs can have similar K_d while having vastly different association constants and dissociation constants. (Singhal et al.,

2010) Short time scales are critically important when developing POC tests. An end-user ought to receive results within a few minutes, so binding kinetics on short timescales will be more relevant than the longer timescales pertinent to equilibrium binding.

How rapidly two entities bind to each other is characterized by the kinetic rate constant k_{on} [units $\frac{L}{mol\ s}$] The lower the k_{on}, the faster the two entities bind each other. Conversely, the rate constant k_{off} [units s^{-1}] measures how quickly a bound pair will dissociate from each other. The lower the k_{off} the stronger the paired moieties bind each other.

Mechanisms for enhancing signal

Signal types also influence the design and reproducibility of a lateral flow test. Colorimetric labels are the most visually apparent type of labels used for lateral flow tests and are conducive to simple device fabrication and construction for a point-of-care device. This study will investigate three varieties of colorimetric signals: gold nanoparticles, cellulose nanoparticles, and horseradish peroxidase coupled with diaminobenzidine substrate.

For the final stages of device refinement, blood plasma samples will be collected from infants via venipuncture collection. The typical volume one can reasonably obtain from an infant venipuncture is 1 mL or less. (WHO, 2010) This presents a challenge to enhance signal from a limited sample volume. Instead of increasing the volume of sample processed, this study will focus on the marginal signal gains from a constant, small sample volume. We will explore the effects of increasing mass flux locally via geometric constrictions, as well as examining different colorimetric particle labels and enzymatic labels mentioned previously.

Chapter 2: Signal enhancement by geometric manipulations

A. Introduction and background

Two of the main challenges in lateral assay development are decreasing the limits of detection (LOD) and increasing the ratio of signal from a true positive result to the background signal, also called background-normalized signal (BNS). To improve visual detection limits it is crucial to increase the darkness of a signal relative to its immediate background; signal gains are lost when the background noise increases proportionally to the signal of a true positive. The intensity of a positive test signal depends on the amount of analyte present and the time with which other assay components interact and bind with their respective pair(s). Component concentrations in sample as well as the flow velocity of sample through the porous matrix affect how easily and how well components can bind each other and remain bound.

A lateral flow strip can be geometrically altered to modify fluidic behavior along its flow path. Mass flux increases are one way in which BNS can be enhanced by constricting the geometric pathway along a continuous flow field. When a fluid flows through a region of low pressure, the flow velocity increases; vice-versa when a fluid flows through a region of high pressure.

(Zadehkafi et al., 2019) demonstrated this phenomenon using a lateral flow test strip architecture that tapered downstream. With sample size held constant, they found that tapering the flow matrix downstream increased the BNS after normalizing for area. This was consistent across all antigen concentrations. However, the tapered geometries of the strips result in unequal areas of porous media among test strip architectures. Their test line location remained constant, but the total flow path area was not.

(Parolo et al., 2013) investigated similar effects on BNS by manipulating the size and geometry of the sample pad rather than directly modifying the lateral flow strip. Parolo and researchers found substantial decreases in the LOD when sample size and conjugate label were increased commensurately. This mechanism does not work well when sample size is a limiting factor, as it is in infant HIV diagnosis. Our sample is extracted from a small heel prick on an infant, so our sample size is a significant limiting factor. Signal enhancement by increasing sample size may not be practical for BNS enhancement in our assay.

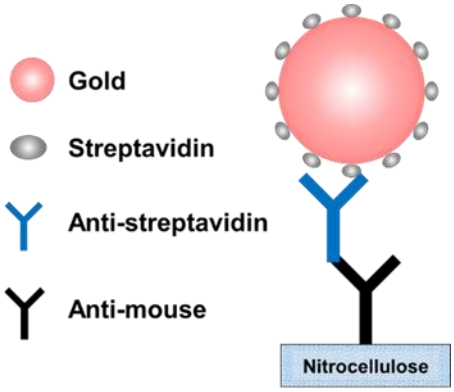

Figure 1. *Schematic of model assay sandwich used to assess signal gains in constricted regions of detection. An anti-mouse antibody on nitrocellulose captures an anti-streptavidin antibody. Streptavidin-gold conjugate label is used to visualize the capture event.*

We propose a combination of the two approaches mentioned previously: Using a model antibody sandwich, we want to observe the potential BNS enhancement by locally increasing mass flux through a region of interest, that is, our capture antibody test line. This results in a more uniform flow path where the constriction is localized only in relevant regions, thus preserving more uniformity along most of the flow path. We will keep our small sample volume constant (50 μL) for practical reasons, however localized constriction increases the mass flux through the detection region of interest. This allows us to mimic the effects of increased mass flux through the lateral flow strip as (Parolo et al., 2013) demonstrated. We predict that, due to the high binding constants among pairs in our model antibody sandwich that the localized

increase in flow velocity will not cause an equal reduction in signal gains from increased localized mass flux.

B. Methods and materials

i. Reagent information

Design of device components were constructed using a drafting software package, DraftSight (Dassault Systemes, Waltham MA.) Excision of test strip components was performed using a laser cutter, at power and speed settings appropriate for the material used. For the model assay test strips, nitrocellulose was cut to 25 mm x 6 mm overall, with localized constriction widths ranging from 6 mm (uniform), 3 mm, and 1.5 mm.

Capture antibody was deposited onto nitrocellulose matrix using a nanoaspirator (BioDot, Model AD2200, Anaheim CA) at a deposition rate of 1.0 μL/cm. The strips with deposited capture antibody were dried overnight in a desiccator. *Biologicals* Capture antibody: Goat source anti-mouse mAb; solution concentration: 1.5 mg/mL; aspiration rate: 1.0 uL/cm (Vector laboratories, Burlingame CA). Antigen: Mouse source anti-streptavidin mAb; solution concentration: 25 ng/mL (Abcam, Cambridge MA). Streptavidin-Gold, 60 nm diameter, prepared to OD1 (Arista Biologicals, Allentown PA)

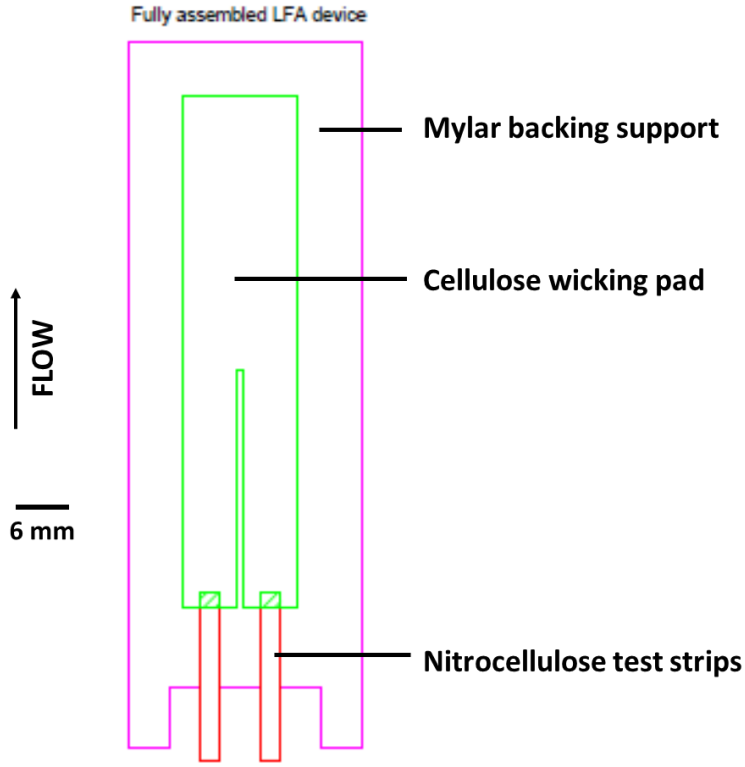

Figure 2. *Schematic of fully assembled lateral flow assay card. Nitrocellulose test strips are placed backing side down onto a plastic support base with adhesive. The wicking pad is placed atop the nitrocellulose strips with exactly 2 mm overlap. The fully assembled card is then sealed with spacers and a top cove (not shown).*

ii. Lateral flow strip processing

The strips are then passivated against nonspecific adsorption using a blocking solution of casein (1 % w/w) and polysorbate-20 (0.05 % v/v) in 10 mM phosphate buffer solution (PBS) for 1 hour at ambient temperature under gentle agitation. The passivated strip is then washed 3 times for 8 minutes using fresh PBS each wash cycle. The strip is dried in a desiccator for at least 2 hours before assaying.

Assay cards are constructed by applying manually individual strips aligned to the bottom of the card with the plastic backing side down. An absorbent pad is then aligned and applied to

the same card so that the bottom of the absorbent pad is aligned 2 mm from the top of the strip. Spacer strips are applied to the sides of the card to provide space for absorbent pad and sealed with a top sheet of mylar for a semi-closed system. This dipstick architecture allows us to operate lateral flow tests without sample pads; the card can be positioned upright in a 96-well plate for easy fluid application.

To process the lateral flow assay, first a wash is applied to the nitrocellulose matrix to establish fully wetted flow, Next , a solution of antigen and label, previously mixed before application to matrix, is applied to fully wetted matrix. A final wash is applied for increased background clearance.

Table 1. *Assay component addition sequence for model stack with streptavidin-gold label.*

Assay component	Component Name	Volume applied
1. *Wash*	*PBST* (0.05%)	30 μL
2. *Antigen, Label*	*Anti-Streptavidin IgG* (25 ng/mL), *Streptavidin-Gold* (OD1)	50 μL
3. *Wash*	*PBST* (0.05%)	50 μL

iii. Data analysis

Upon assay completion the processed strips are scanned using a flatbed scanner (Epson, Nigano, Japan) at 16-bit depth, 1600 dpi. Scanned images are then analyzed using a custom MATLAB processing program that obtains the mean grey intensity for a specified region on the image. The user clicks a fiducial mark 2.3 mm down from the detection region of interest to obtain the mean grey intensity. The same fiducial mark obtains a mean grey intensity for the background immediately upstream from the detection region, or 3.3 mm down from the detection region. The area of analysis is 50 x 19 pixels, or 950 square pixels.

Signal analysis was performed by comparing background-normalized signal intensities. The normalized signal was processed using the equation below:

$$\frac{MGV_{back} - MGV_{test}}{MGV_{back}} \times 100\%$$

where MGV_{back} is the mean gray scale value of the background, and MGV_{test} is the mean gray scale value of test line.

C. Results and Discussion

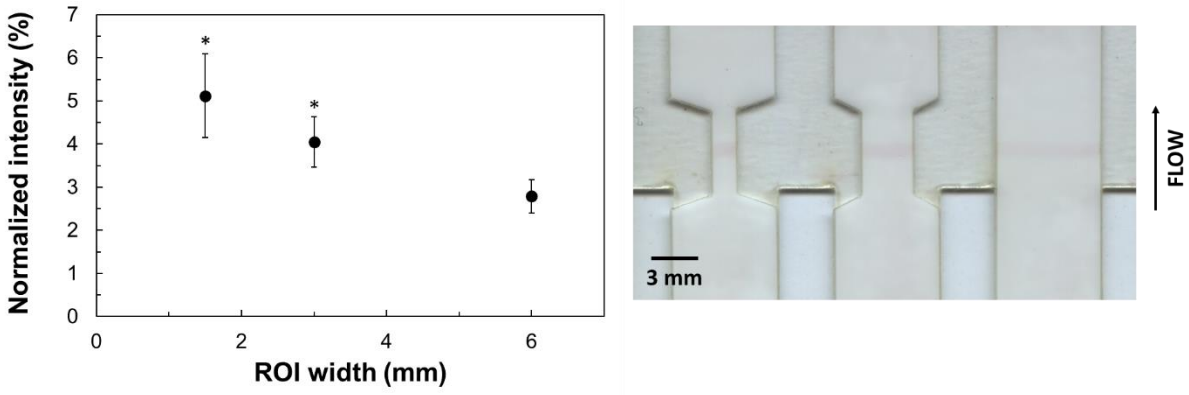

Figure 3. *Localized geometric constriction along lateral flow pathways increases normalized signal intensity at similar antigen levels. (Left) Normalized signal intensities (N = 4) plotted as a function of localized constriction widths 1.5, 3.0, and 6.0 mm, respectively. (Right) Scanned image of lateral flow test strips used to quantify signal gains by localized geometric constriction.*

i. Localized constrictions; signal gains for model antibody system

Using the model antibody system, we found that localized geometric constriction does provide significant increases in normalized signal intensity compared to the uniform strip architecture. Both constricted geometries, 1.5 mm ($p < 0.05$) and 3.0 mm ($p < 0.05$), showed significantly higher BNS compared to that of the uniform 6.0 mm strip. The BNS differences between 1.5 mm detection regions and 3.0 mm detection regions were not significant ($p = 0.05$).

The increased Higher BNS variability in the 1.5 mm systems may contribute to this. In general, signal gains were proportionate to the amount of localized constriction, that is, more constricted regions saw more intense signals. This is consistent with our predictions of increased mass flux encouraging more binding events between antigen and target, and between complex and label on the test strip.

The improvements in normalized signal is a balance between competing forces. The flow velocity is likely high enough to provide additional clearance of nonspecific binding, yielding a cleaner background and higher signal contrast. The flow velocity must also be low enough not to affect the high affinity binding kinetics among the components of the model antibody sandwich.

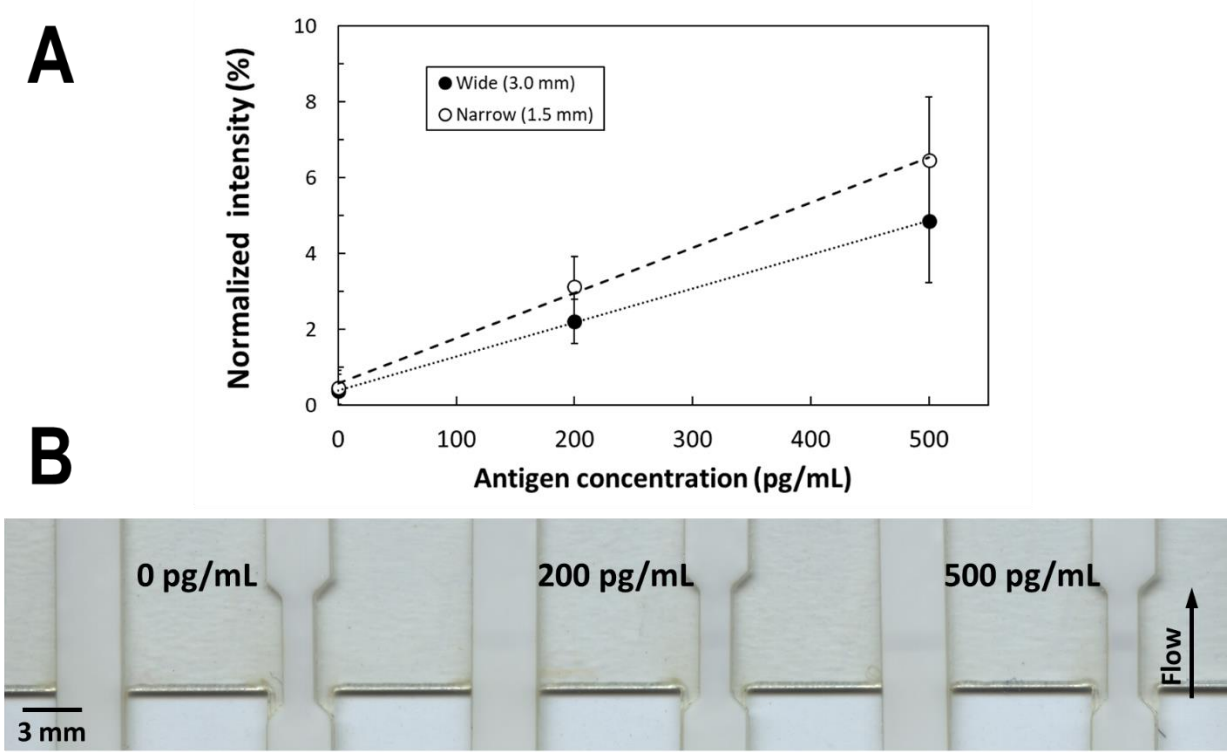

Figure 4. *Demonstration of normalized signal gains from localized geometric constrictions in lateral flow tests using a customized cellulose nanobead label. (A) Normalized signal response plotted as a function of three different antigen concentrations (N = 6), 0, 200, and 500 pg/mL. (B) Scanned images comparing signal intensity from locally constricted strips and uniform strips.*

ii. Localized constrictions; signal gains for HIV system

We compared the normalized signal intensities using a customized cellulose nanobead label (reference Chapter 3) and found no significant differences between strips with localized constrictions along the capture region and strips with uniform flow paths. Due to reagent availability, strips of 3 mm were used rather than the 6 mm baseline width as used in the model system. This may be due to differences in the HIV-sandwich architecture. Although the signal differences were not significant, average signal was still higher on average for locally constricted strip geometries. So, we proceeded in this study using the locally constricted detection regions to operate with the highest normalized signal intensity possible.

To conclude, we have demonstrated that locally constricting the region of detection with a model antibody system can provide significant gains in signal intensity compared to the signal from a uniform flow path. Constricting the region of detection by 50% (6 to 3 mm) yielded a 48 % increase in normalized signal intensity; locally constricting the detection region by 75% (6 to 1.5 mm) resulted in an 82 % increase in normalized signal for a model antibody assay with gold label. Signal gains for the HIV system were not significant when comparing locally constricted to uniform flow paths. We did observe a significant increase in antigen sensitivity by using a different label. This led us to hypothesize that changing the label type from gold to a darker and much larger nanoparticle would help us reach our clinical detection limit goal of 10 pg/mL p24.

Chapter 3: Detection of p24 antigen with colorimetric particles

A. Introduction and background

Colorimetric particle detection is a visually direct method of detection used in lateral flow assays. This ease of signal detection has rendered it one of the most popular ways to label a positive signal in paper-based immunoassays. Colorimetric particle detection requires no external instrumentation to visualize the signal and is user-friendly. These qualities align well with the ASSURED paradigm.

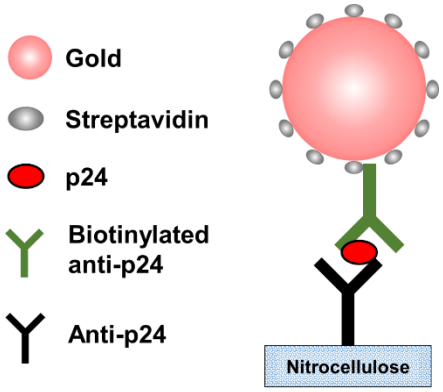

Figure 5. *Schematic of HIV stack with streptavidin-gold labeling. An anti-p24 capture antibody, deposited onto nitrocellulose, captures p24 antigen which has been previously mixed with a biotinylated anti-p24 detection antibody. A solution of streptavidin-gold (OD1) is applied to passivated matrix to visualize capture event.*

Gold nanoparticles are the most commonly used colorimetric particle used in lateral flow detection. Its kinetic behavior, such as interparticle aggregation and immobilization on the porous flow matrix, can be monitored in real time. Gold nanoparticles are well characterized and can be purchased ubiquitously from commercial vendors or made in lab using an auric chloride reduction reaction. The concentration and particle size can be determined directly by UV-vis spectroscopic methods. (Hsieh, Helen V.; Dantzler, Jeffreu L; Weigl, 2017) cite several examples of particle labeling techniques and characterization in LFIAs.

Our HIV assay, pictured in Figure 5, is labeled using a commercially sourced *streptavidin*-gold conjugate which binds to biotin markers on the biotinylated anti-p24 detection antibody. The biotinylated detection antibody is premixed with the p24 antigen before applying to the flow matrix. While gold nanoparticles are ubiquitous and inexpensive, their pink color can make it challenging for end-users to discern a positive signal from the background. This low signal contrast results in a raised limit of detection.

Latex beads are a popular alternative to gold nanoparticles. They are on average an order of magnitude larger in diameter compared to the most commonly used gold nanoparticles and come in a diverse range of colors. This allows for the simultaneous detection of multiple, distinct targets in a single sample. (Zhang et al., 2006) demonstrated the utility of latex beads in a multianalyte immunochromatographic screening assay. This works essentially like a LFIA on porous nitrocellulose matrix. They were able to quantify four distinct nitrofuran metabolites in animal food products to notably low detection levels at hundreds of micrograms per milliliter of sample. Their large size is not always an advantage in LFIAs. Previous work indicates that the significantly large size of latex beads can limit their mobility in a porous matrix. (Linares et al., 2012) indicate that large latex beads can form conglomerates up to 600 nm in diameter.

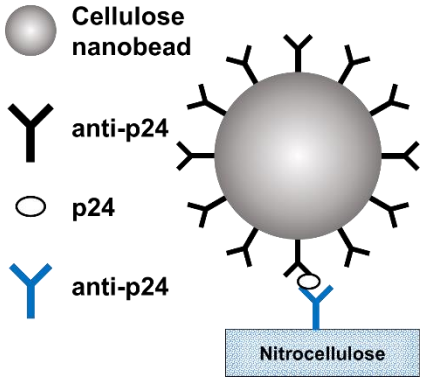

Figure 6. *Schematic of HIV stack with CNB labeling. An anti-p24 capture antibody, deposited onto nitrocellulose, captures p24 antigen which has been previously mixed with CNB label conjugate.*

Cellulose nanobeads have been used as an alternative to latex beads. Although smaller in diameter compared to the latex beads, cellulose nanobeads are still significantly larger than most gold nanoparticle diameters. Compare 200 nm average diameter for cellulose nanobeads to 60 nm average diameter for gold nanoparticles. Our HIV assay labeled with CNB-antibody label, pictured in Figure 6, is constructed by first pre-mixing the CNB-antibody label solution with p24 antigen before applying to the porous matrix; p24 is captured by the immobilized anti-p24 capture antibody. The black color of the cellulose nanobeads contrasts nicely with the white background of our nitrocellulose porous matrix. Enhanced contrast improves signal visibility and can decrease visual limits of detection. (Sakurai et al., 2014) quantified the signal gains in visual signal detection in influenza viral detection assay in lateral flow format. They found a 10-fold decrease in LOD using cellulose nanobeads compared to colloidal gold and colored latex beads. In this chapter, we explore and compare the LOD of an HIV sandwich assay using traditional colloidal gold nanoparticles conjugated to *Streptavidin* and using cellulose nanobeads conjugated to anti-p24 detection antibody. We anticipate similar improvements to LOD as seen by Sakurai *et al.*

B. Materials and methods

i. Reagent information

Streptavidin-gold conjugate (Arista Biologicals, OD10) was diluted 10:1 v/v with PBST (0.05% polysorbate-20). A commercially purchased EZ-Link™ NHS-PEG4 Biotinylation kit (ThermoFisher) was used to conjugate biotin moieties to the anti-p24 detection antibody. Briefly, a solution of NHS-PEG4 Biotin was prepared from a freeze-dried sample to 8.5 mM with PBS (10 mM) containing no K^+ ions. NHS-PEG4-Biotin solution was mixed with anti-p24 detection

antibody at a ratio of 40-fold molar excess of biotin and allowed to sit at ambient temperature for 30 minutes. The solution is then filtered through a size-exclusion column. The extent of biotinylation was quantified using a commercially purchased Biotin Quantification Kit (ThermoFisher.) On average, per anti-p24 detection antibody there were 13 +/- 2 biotin moieties attached.

ii. Cellulose nanobead label conjugation

A commercially purchased cellulose nanobead conjugation kit (DCN Diagnostics, Carlsbad CA) was used to conjugate our anti-p24 detection antibody. Briefly, a solution of cellulose nanobeads was mixed with our anti-p24-antibody solution at a bead-to-protein mass ratio 10:1 for 1 hour at 37 *C while gently agitating. The conjugated nanobeads were passivated with a proprietary blocking buffer at 37 *C for 2 hours while gently agitating. The conjugate was purified via centrifugation and resuspended in PBS to a final concentration of 0.2% w/w.

iii. Lateral flow strip processing

Using a BioDot nanoaspirator, anti-p24 capture antibody (1.0 mg/mL) was deposited onto nitrocellulose (1.0 uL/cm) and allowed to dry overnight in a desiccator. Strips with antibody were nonspecifically blocked in a casein (1%) blocking buffer solution for 1 hour at ambient temperature. Individual strips, as well as other assay card components, were excised using a CO_2 plasma laser cutter (Scottsdale AZ) and assembled onto a custom excised card with an adhesive backing.

Table 2. Assay component addition schedule for HIV assay with streptavidin-gold labeling. Replicates (N = 4) were performed for four distinct p24 antigen concentrations.

Assay component		Component contents	Volume applied
1.	*Wash*	*PBST* (0.05%)	30 μL
2.	*Premixed antigen*	▪ *Biotinylated detection IgG* (c_f = 100 μg/mL) ▪ *P24 antigen*	50 μL
3.	*Conjugate label*	*Streptavidin-Gold* (OD1)	50 μL
4.	*Wash*	*PBST* (0.05%)	50 μL

Once the cards were fully assembled, they were placed with the nitrocellulose tabs inserted into individual wells of a 96-well plate. First, a wash is applied to the nitrocellulose to establish fully wetted flow. Then, a solution of antigen and biotinylated detection antibody is let to mix for 5 minutes before applying to the matrix. Next, a solution of streptavidin-gold is applied to generate a colorimetric signal. A final wash of PBST is applied to improve background clearance. Additional details are listed in Table 2. Assay component addition schedule for HIV assay with streptavidin-gold labeling. Replicates (N = 4) were performed for four distinct p24 antigen concentrations.

iv. Data processing

Test strips were scanned on a flatbed scanner (Perfection V700 Photo, Epson, Nagano, Japan) after assay completion. Images were scanned at 16-bit depth, 1600 dpi pixel density. The normalized signal was processed using a custom MATLAB script by selecting a fiducial mark located on the strip's left edge 2.3 mm down from detection region. The background is obtained from a region of identical size and orientation (950 sq pixels) immediately upstream from the

capture region. Statistical calculations were performed using a two-tailed student t-test assuming unequal variance.

v. Calculations: Limit of detection

We also compare the concentration LOD by assessing low-level noise. The equation below outlines the concentration LOD metric:

$$LOD = \frac{[\mu_{blank} + 1.645(\sigma_{blank} + \sigma_{low})] - b}{m}$$

where μ_{blank} is the average normalized signal of antigen blank samples, σ_{blank} is the variance of antigen blank samples, σ_{low} is the variance of lowest non-zero antigen sample, b is the y-intercept of linear fit to response curve, and m is the slope of linear fit to response curve

C. Results and discussion

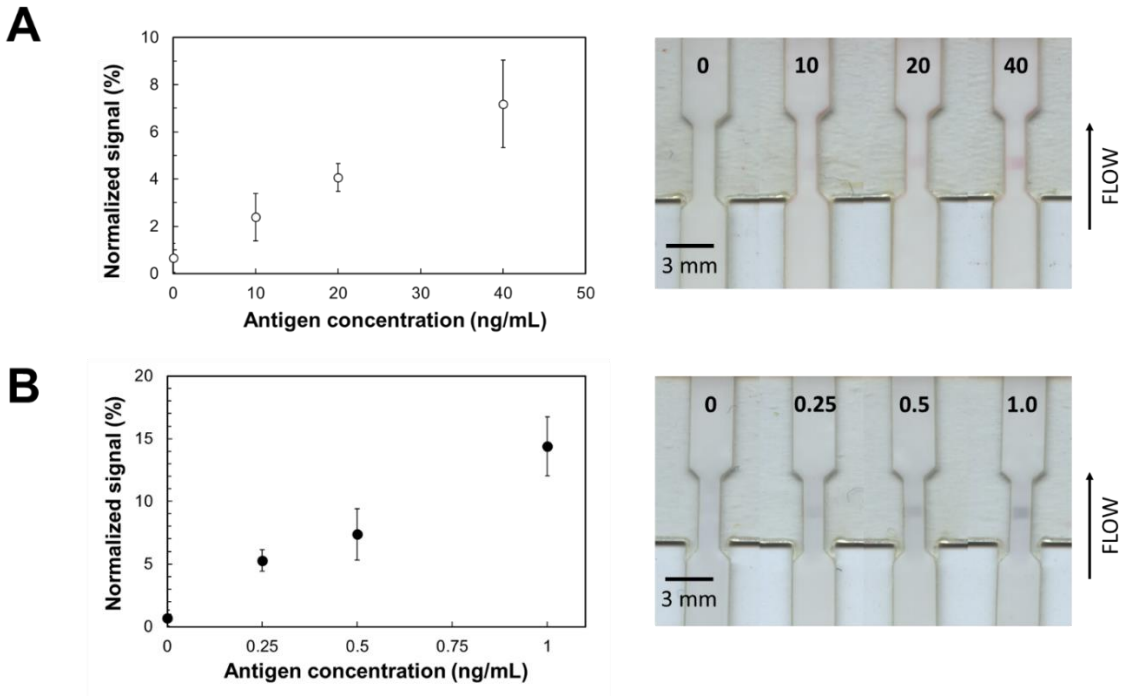

Figure 7. *Signal response curves for particle detection methods in HIV p24 assay. Error bars rep one standard deviation from mean (N = 4). Signal response shown only for constricted geometries. (A) (left) Plot of signal response for HIV assay labeled with streptavidin-Gold nanoparticles. (right) Representative assay strips at 0, 10, 20, 40 ng/mL p24, region of interest in centered in constricted geometry. LOD = 19 ng/mL (B) (left) Plot of signal response for HIV assay labeled with CNB-antibody labels. (right) Representative assay strips at 0, 0.25, 0.5, 1.0 ng/mL p24, region of interest is centered in constricted geometry. LOD = 150 pg/mL.*

Because we observed higher average signal intensities with constricted flow systems compared to uniform flow systems, we decided to compare signal intensities using different labels only in the constricted systems. It was determined in other experiments not discussed in this chapter that there were in fact no significant differences in signal between uniform and constricted systems when performing our HIV sandwich immunoassay.

Comparing model antibody sandwich to HIV antibody sandwich

We observed similar signal intensity for the HIV system labeled with gold to the that in the model antibody system. Both systems appear linear with CNB-antibody label providing the higher signal intensity than colloidal gold. The concentration LOD using *streptavidin*-gold

nanoparticles was calculated at 19 ng/mL p24 for constricted systems of our HIV immunoassay. For our HIV assay using CNB-antibody label the LOD was 150 pg/mL p24, an order of magnitude lower than the equivalent assay labeled with gold. It is critical to note that, while we were successful in lowering our LOD with the CNB-antibody label, it was not sufficient to reach our clinical target LOD of 10 pg/mL. Furthermore, despite the decrease in LOD by two orders of magnitude, a single order of magnitude greater than the findings of (Sakurai et al., 2014), these two antibody sandwich stacks are not identical in construction.

While the capture antibody deposited on the porous matrix and source of antigen are identical, the HIV assay labels capture events by premixing with a biotinylated anti-p24 antibody Both immunoassays, the model antibody system and the HIV sandwich immunoassay, used the same gold label in similar concentrations. However, the model system had a strip uniform width of 6 mm that constricted the width immediately surrounding the detection region locally; the HIV system had a strip uniform width of 3 mm that, like the model antibody system, constricted the detection region locally. The model system has an immunosandwich architecture that involves the binding of an anti-streptavidin epitope on the secondary antibody and streptavidin on the colloidal gold label. This limits the number of anti-streptavidin epitopes available to just two for every capture event, but the large size of the gold nanoparticles compared to the antibody indicate that sterics limit the number of label particles per binding event. Additionally, processing additional bulk fluid can contribute to lost signal, albeit at a comparatively low rate, resulting from interrupting the interaction between antigen and capture antibody or biotinylated detection antibody and antigen. This can reduce the assay's final signal intensity. In contrast, the HIV immunosandwich architecture involves binding between biotin on the biotinylated detection antibody and streptavidin on colloidal gold nanoparticles. A biotinylated detection antibody

presents approximately 12 biotin markers per detection antibody as determined by a competitive HABA reaction using spectroscopic techniques. The biotin markers are estimated to be well dispersed along the surface of the detection antibody providing several more potential labeling targets for streptavidin. This greatly increases the number of labeled binding events in the HIV assay. Therefore, it is impressive that despite having additionally more potential biding sites for labeling the gold system is outperformed by the CNB system.

There is some evidence to suggest that the increase in signal intensity is at least assisted by not an intrinsic boost in positive signal, but a boost in background clearance in constricted flow geometries (see Appendix). The added contrast that CNBs present against a white background would deliver a definitive positive signal with as much visual contrast as possible. The pink color of colloidal gold does not provide optimal contrast against a white background such as a porous nitrocellulose matrix. While it is not definitive which factors contributed to higher signal intensity with the CNB-antibody label (better contrast or more direct detection stack), direct particle detection with colorimetric particles may not be sufficient to reach our clinical LOD of 10 pg/mL p24. Signal amplification could provide us with the additional boost needed to achieve our target LOD.

Chapter 4: Detection of p24 antigen with horseradish peroxidase

A. Introduction and background

Enzyme amplification is a method used to enhance the visual detection of a target using a secondary enzyme that binds an immobilized target. The enzyme's respective substrate is then introduced; the interaction between substrate and enzyme generates an insoluble colored substance at the site of target capture.

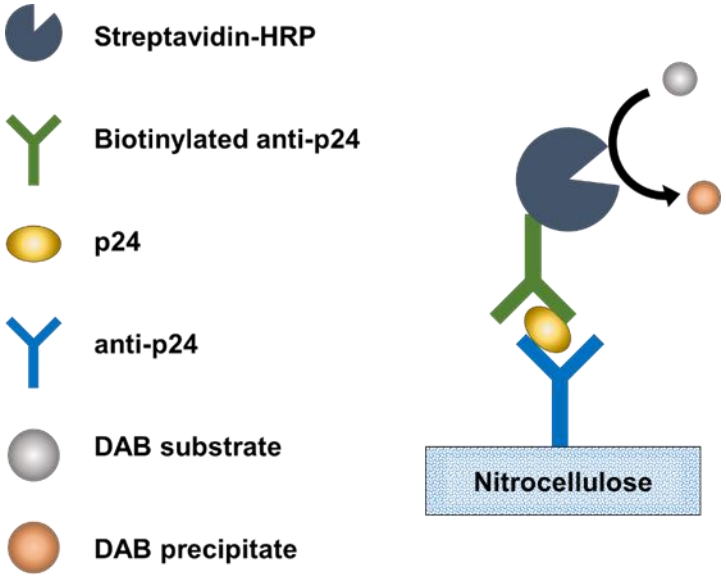

Figure 8. *Schematic of HIV stack with HRP amplification. An anti-p24 capture antibody, deposited onto nitrocellulose, captures p24 antigen, which has been previously mixed with biotinylated anti-p24 detection antibody. Streptavidin-HRP binds to the biotinylated anti-p24 antibody. Diaminobenzidine (DAB) then reacts with HRP to produce a brown, insoluble precipitate.*

In our specific antibody sandwich, a biotinylated anti-p24 detection antibody is mixed with p24 antigen for two minutes in solution prior to matrix application. This mixture is then applied to the matrix and flows through the capture region where p24 antigen is immobilized A separate solution of HRP is processed through the matrix where it binds biotinylated anti-p24 detection antibody and becomes immobilized in the capture region, as well. A wash solution is applied after HRP to minimize nonspecific reaction outside the capture region.

Diaminobenzidine (DAB) is then activated with an oxidizing solution and applied to the matrix where it interacts with immobilized enzyme, generating an insoluble brown precipitate.

Enzyme amplification has been used extensively to enhance the signal sensitivity of immunoassays with notable success. This improvement in signal sensitivity is especially attractive in assays designed to detect small molecules at nanomolar concentrations (C. C. Chiou et al., 2003). Studies have quantified the signal gains from an enzyme amplification as compared to direct particle label detection indicating that an approximate 5-fold improvement in LOD with amplification can be expected (Goryacheva et al., 2008). Ramachandran et al. have demonstrated a 5-fold signal improvement in a well-behaved malarial assay using enzyme amplification in nitrocellulose. Our device design was inspired by their flow path design includes a wash separating the enzyme and substrate as they flow along the porous matrix.(Ramachandran et al., 2014)

These examples demonstrate that enzyme amplification, specifically HRP, is a robust technique that can provide signal boosts where limits of detection are low. We believe exploring HRP amplification coupled with DAB substrate holds promise to reach our clinical detection limit of 10 pg/mL.

B. Methods and materials

i. Reagent information

Streptavidin-Horseradish peroxidase (ThermoFisher, Catalog No 21130) was prepared to 1 μg/mL with 10 mM PBS and 0.05 % polysorbate-20. Diaminobenzidine (ThermoFisher,

Catalog No 34002) was prepared to 1x by diluting concentrated DAB with hydrogen peroxide catalytic solution just before processing.

ii. Assay sequence

A wash is first applied to the nitrocellulose matrix to establish fully wetted flow. Next, a solution of antigen and biotinylated detection antibody, previously mixed before application to matrix, is applied once the wash solution is completely imbibed. A solution of streptavidin-HRP is applied to the matrix once premixed solution has been fully imbibed. An intermediate wash is applied to physically separate the substrate from interacting with HRP in areas extraneous to detection region. A substrate of hydrogen peroxide and DAB is prepared fresh immediately before application to 1x strength. Lateral flow assay is complete once substrate has been fully imbibed. Strips are scanned within 10 minutes of full imbibement

Table 3. *Assay component addition sequence for HIV stack with biotinylated detection antibody and HRP amplification.*

Assay component	Name	Concentration	Volume applied
1. Wash	PBST/casein	-	30 µL
2. Antigen	P24	≤ 1'000 pg/mL	30 µL
Detection antibody	Biotinylated IgG	10 ug/mL	
3. Enzymatic label	SA-HRP	1 ug/mL	40 µL
4. Wash	PBST/casein	-	30 µL
5. Enzyme substrate	Diaminobenzidine	1x	40 µL

C. Results and discussion

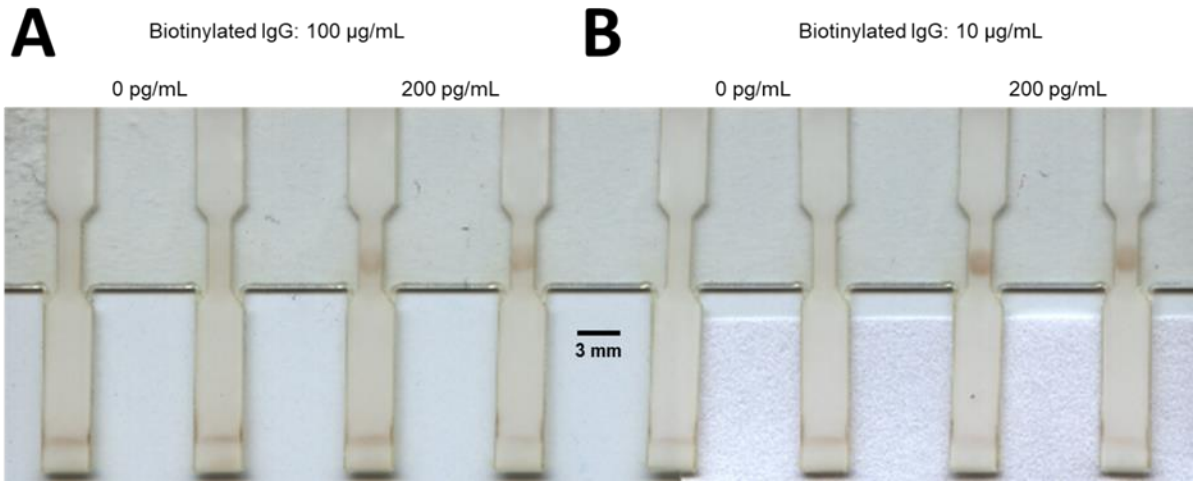

Figure 9. *Signal improvements from reduction of detection antibody load. (A) Signal generation in system containing biotinylated detection antibody at 100 µg/mL. (B) Signal generation in system containing biotinylated detection antibody at 10 µg/mL. Concentrations listed just above strips indicates p24 antigen concentration. Streptavidin-HRP was prepared to 1 µg/mL and then applied to the strips. DAB was prepared fresh to 1x concentration with peroxide solution immediately before application to strips.*

In our initial studies of the HRP amplification system, we found that decreasing the concentration of biotinylated detection antibody (**Figure 9**) and streptavidin-HRP improved assay signal LOD evidenced by increased visibility on the test strip surface. While increasing the effective concentration of the p24 antigen may be responsible for signal gains, there is evidence that the matrix becomes clogged with excess reagent and prohibits signal generation downstream in the detection region.

Using enzymatic amplification to increase assay signal sensitivity presents additional challenges to achieving a POC device for early p24 detection. Compared to colorimetric particles which are visually apparent from the surface of a porous matrix once bound to its respective target, enzymatic labels require more than one reagent in sequential combination to produce a signal visible by the naked eye. Specifically, DAB solution must be prepared fresh with a peroxide solution immediately before application to the matrix. The peroxide solution provides the oxidant necessary for precipitate formation. (Ramachandran et al., 2014) demonstrated a two-

dimensional paper network that would allow the sequential delivery of enzyme, substrate, and catalyst along a single flow-path. They showed successfully that you could dry the reagents needed for the amplification reaction and, upon hydration from a liquid sample, could carry out a HRP amplified reaction on a porous matrix for immuno-type assays. In all our HRP amplified test strips, nonspecific signal generation was still observed at the bottom of each strip despite the addition of a buffer wash between enzyme application and substrate application. This may be due to continued oxidation of DAB by the peroxide solution. Areas outside the capture region on test strips did not display this severe nonspecific signal production, which helped preserve the contrast between amplified signal in the capture region and its immediate upstream background. In this study we use a simple half-dipstick format to execute assays. This simple design makes it difficult to incorporate other complex pathways for separate substrate introduction. Consequently, DAB and peroxide solution were prepared fresh as directed and introduced by manual fluid transfer.

Even with tightly controlled and appropriate reagent delivery, there remains a critical narrow time frame when amplified signal response is proportional to the amount of antigen detected. Outside this time frame, signal becomes oversaturated due to continued precipitate formation as time elapses. Using a stop solution, as done in ELISA, cannot be as practically implemented into a lateral flow device. Stop solutions present two problems: the first problem is introducing additional user steps to process POC test results increases the likelihood of inaccurate or inappropriate assay execution, the second problem is the introduction of a stop solution could permanently alter the colorimetric signal so that the end user has difficulty interpreting the results. Because it is not practical to stop the amplification reaction once it has begun *in situ* the results are interpreted within five minutes after fully imbibing the substrate

solution. Although interpreting a tightly timed assay is feasible in a laboratory setting, it presents an opportunity for improvement when developing a final POC device with an enzyme amplification system. The development of an amplification system that stops after a specified time would be ideal to capture the amplified signal in a visible, linear range.

In this study, only constricted geometries were used with the HRP amplification system. It was decided, from previous studies, that the constricted geometry could yield the highest gains in signal on our test strips. While our goals were focused on reaching our clinical LOD at 10 pg/mL, it would be valuable to assess what affect geometric manipulation has on a colorimetric signal from enzyme amplification. Similarly, combing the effects of a colorimetric particle label with enzymatic amplification is an alternative avenue to enhancing apparent signal. (Zhang et al., 2006) demonstrated a significant improvement in LOD for detecting small, broad spectrum insecticides by combing colorimetric tracer particle labels with HRP amplification. Using only colorimetric particle labels their initial LOD ranged from 10-100 ug/mL, using a combination of particle label and enzyme amplification their LOD reduced to 1-10 ug/mL. Our assay signal detection limit could reasonably be reduced near 1 pg/mL given the clear signal at 10 pg/mL using HRP amplification (**Figure *9***).

Works Referenced

Chiou, C. C., Chang, P. Y., Chan, E. C., Wu, T. L., Tsao, K. C., & Wu, J. T. (2003). Urinary 8-hydroxydeoxyguanosine and its analogs as DNA marker of oxidative stress: Development of an ELISA and measurement in both bladder and prostate cancers. *Clinica Chimica Acta*. https://doi.org/10.1016/S0009-8981(03)00191-8

Chiou, M., Goulet, D., Teplyakov, A., & Gilliland, G. (2019). Antibody Structure and Function : The Basis for Engineering Therapeutics. *Antibodies*, *8*(55), 1–80.

Fritz, F., Tilahun, B., & Dugas, M. (2015). Success criteria for electronic medical record implementations in low-resource settings: A systematic review. *Journal of the American Medical Informatics Association*, *22*(2), 479–488. https://doi.org/10.1093/jamia/ocu038

Gomez, I. J., Arnaiz, B., Cacioppo, M., Arcudi, F., & Prato, M. (2018). Nitrogen-doped Carbon Nanodots for bioimaging and delivery of paclitaxel. *Journal of Materials Chemistry B*, *6*(35), 1569–1580. https://doi.org/10.1039/x0xx00000x

Goryacheva, I. Y., Beloglazova, N. V., Eremin, S. A., Mikhirev, D. A., Niessner, R., & Knopp, D. (2008). Gel-based immunoassay for non-instrumental detection of pyrene in water samples. *Talanta*, *75*(2), 517–522. https://doi.org/10.1016/j.talanta.2007.11.042

Hsieh, Helen V.; Dantzler, Jeffreu L; Weigl, B. H. (2017). Analytical Tools to Improve Optimization Procedures for Lateral Flow Assays. *Diagnostics*, *7*(2), 29. https://doi.org/10.3390/diagnostics7020029

Lin, G. G., Zhao, G., Perilla, J. R., Scott, J. G., Yufenyuy, E. L., Meng, X., Chen, B., Ning, J., Ahn, J., Gronenborn, A. M., Schulten, K., Aiken, C., & Zhang, P. (2012). Mature HIV-1 capsid structure by cryo-electron microscopy and all-atom molecular dynamics. *Nature*, *100*(2), 130–134. https://doi.org/10.1016/j.pestbp.2011.02.012.Investigations

Linares, E. M., Kubota, L. T., Michaelis, J., & Thalhammer, S. (2012). Enhancement of the detection limit for lateral flow immunoassays: Evaluation and comparison of bioconjugates. *Journal of Immunological Methods*. https://doi.org/10.1016/j.jim.2011.11.003

Martinez, A. W., Phillips, S. T., Whitesides, G. M., & Carrilho, E. (2010). Diagnostics for the developing world: Microfluidic paper-based analytical devices. *Analytical Chemistry*, *82*(1), 3–10. https://doi.org/10.1021/ac9013989

Mendez, S., Fenton, E. M., Gallegos, G. R., Petsev, D. N., Sibbett, S. S., Stone, H. A., Zhang, Y., & López, G. P. (2010). Imbibition in porous membranes of complex shape: Quasi-stationary flow in thin rectangular segments. *Langmuir*, *26*(2), 1380–1385. https://doi.org/10.1021/la902470b

Miedouge, M., Grèze, M., Bailly, A., & Izopet, J. (2011). Analytical sensitivity of four HIV combined antigen/antibody assays using the p24 WHO standard. *Journal of Clinical Virology*, *50*(1), 57–60. https://doi.org/10.1016/j.jcv.2010.09.003

Parolo, C., Medina-Sánchez, M., De La Escosura-Muñiz, A., & Merkoçi, A. (2013). Simple paper architecture modifications lead to enhanced sensitivity in nanoparticle based lateral flow immunoassays. *Lab on a Chip*, *13*(3), 386–390. https://doi.org/10.1039/c2lc41144j

Peters, A., & Durner, W. (2008). A simple model for describing hydraulic conductivity in unsaturated porous media accounting for film and capillary flow. *Water Resources Research*, *44*(11), 1–11. https://doi.org/10.1029/2008WR007136

Ramachandran, S., Fu, E., Lutz, B., & Yager, P. (2014). Long-term dry storage of an enzyme-based reagent system for ELISA in point-of-care devices. *Analyst*, *139*(6), 1456–1462. https://doi.org/10.1039/c3an02296j

Rich, K. C., Janda, W., Kalish, L. A., Lew, J., Hofheinz, D., Landesman, S., Pitt, J., Diaz, C., Moye, J., & Sullivan, J. L. (1997). Immune complex-dissociated p24 antigen in congenital or perinatal HIV infection: role in the diagnosis and assessment of risk of infection in infants.(Statistical Data Included). *Journal of Acquired Immune Deficiency Syndromes and Human Retrovirology*, *15*(3), 198.

Routy, J. P., Cao, W., & Mehraj, V. (2015). Overcoming the challenge of diagnosis of early HIV infection: A stepping stone to optimal patient management. *Expert Review of Anti-Infective Therapy*, *13*(10), 1189–1193. https://doi.org/10.1586/14787210.2015.1077701

Sakurai, A., Takayama, K., Nomura, N., Yamamoto, N., Sakoda, Y., Kobayashi, Y., Kida, H., & Shibasaki, F. (2014). Multi-colored immunochromatography using nanobeads for rapid and sensitive typing of seasonal influenza viruses. *Journal of Virological Methods*, 62–68. https://doi.org/10.1016/j.jviromet.2014.08.025

Singhal, A., Haynes, C. A., & Hansen, C. L. (2010). *Microfluidic Measurement of Antibody - Antigen Binding Kinetics from Low-Abundance Samples and Single Cells*. *82*(20), 8671–8679. https://doi.org/10.1021/ac101956e

Slagle, K. M., & Ghosn, S. J. (2018). *Immunoassays: Tools for Sensitive , Specific , and Accurate Test Results*. *27*(3), 177–183.

UNICEF. (2019). *Global and regional trends - HIV*. https://data.unicef.org/topic/hivaids/global-regional-trends/

United Nations Programme on HIV/AIDS (UNAIDS). (2010). UNAIDS Report on the global AIDS epidemic, 2010. In *Unaids*. papers2://publication/uuid/4467B415-2E9B-472A-89EF-B30E692EFE5C

Washburn, E. W. (1921). The Dynamics of Capillary Flow. *Phys. Rev.*, *17*(3), 273–283. https://doi.org/10.1103/PhysRev.17.273

Whitesides, G. M., Kane, R. S., Takayama, S., Ostuni, E., & Ingber, D. E. (1999). Patterning proteins and cells using soft lithography. In D. F. Williams (Ed.), *The Biomaterials: Silver Jubilee Compendium* (pp. 161–174). Elsevier Science. https://doi.org/https://doi.org/10.1016/B978-008045154-1.50020-4

WHO. (2010). WHO guidelines on drawing blood : best practices in phlebotomy. *Pediatric and Neonatal Blood Sampling*.

WHO. (2015). World Malaria Report: 2012. Geneva: WHO, 2012. *Fecha de Consulta*, *23*, 247.

Zadehkafi, A., Siavashi, M., Asiaei, S., & Bidgoli, M. R. (2019). Simple geometrical modifications for substantial color intensity and detection limit enhancements in lateral-flow immunochromatographic assays. *Journal of Chromatography B: Analytical Technologies in the Biomedical and Life Sciences*, *1110–1111*(August 2018), 1–8. https://doi.org/10.1016/j.jchromb.2019.01.019

Zhang, C., Zhang, Y., & Wang, S. (2006). Development of multianalyte flow-through and lateral-flow assays using gold particles and horseradish peroxidase as tracers for the rapid determination of carbaryl and endosulfan in agricultural products. *Journal of Agricultural and Food Chemistry*, *54*(7), 2502–2507. https://doi.org/10.1021/jf0531407